

DEVELOPMENT OF A DISCRETE-TIME AERODYNAMIC MODEL FOR CFD-BASED AEROELASTIC ANALYSIS

Timothy J. Cowan* and Andrew S. Arena, Jr.†
Mechanical and Aerospace Engineering Department
Oklahoma State University
Stillwater, OK 74078

Kajal K. Gupta‡
NASA Dryden Flight Research Center
Edwards, CA 93523

Abstract

System identification is used to develop an accurate and computationally efficient discrete-time aerodynamic model of a three-dimensional, unsteady CFD solution. This aerodynamic model is then used in place of the unsteady CFD solution in a coupled aeroelastic analysis resulting in a substantial savings in computational time. The methodology has the advantage of producing an explicit mathematical relationship for the aerodynamic forces acting on a structure while still retaining the accuracy of the complete unsteady CFD solution. The explicit aerodynamic model can then be coupled with the known structural model and recast in state-space form. Using the combined state-space form, stability and control analysis for the aeroelastic system can be completed based on an eigenvalue solution for the state matrices. Results address the extent to which this methodology is applicable to aerospace applications.

Nomenclature

ρ = free stream density
 a = free stream speed of sound
 CFD = Computational Fluid Dynamics
 $[C]$ = generalized damping matrix
 f = frequency
 \mathbf{f}_a = generalized aerodynamic force vector
 $[I]$ = identity matrix
 $[K]$ = generalized stiffness matrix
 $[M]$ = generalized mass matrix
 M = Mach number
 nr = number of roots or mode shapes
 q = free stream dynamic pressure
 \mathbf{q} = generalized displacement vector

* Graduate Research Assistant, Student Member AIAA.

† Assistant Professor, Senior Member AIAA.

‡ Aerospace Engineer, Member AIAA.

Copyright © 1999 by Timothy J. Cowan and Andrew S. Arena, Jr.. Published by the American Institute of Aeronautics and Astronautics, Inc., with permission.

Introduction

Predicting instabilities in the aeroelastic behavior of aerospace structures is important in the design of modern aircraft which operate over a wide envelope. However, a complete aeroelastic analysis is often difficult to complete due to the complex structural, aerodynamic, and control interactions associated with even the simplest flight vehicles. In order to obtain the most accurate predictions for aircraft flight characteristics, contemporary research has turned toward the development of an integrated computational model capable of capturing these complex interactions.

One of the most powerful computational tools available for aerodynamic analysis is the CFD model. Such a model is often desirable for advanced aerospace applications since it makes the fewest assumptions about the characteristics of the flow field and is capable of accurately predicting complex shock interactions for transonic and supersonic flows around a complicated three-dimensional geometry. For aeroelastic analysis, one can take advantage of these benefits by coupling an unsteady Euler or Navier-Stokes CFD algorithm to an accurate structural dynamics solver and predict the complete aeroelastic response of a structure. However, the computational time required for a CFD-based aeroelastic simulation has typically limited the use of such models in an operational environment even with recent advances in CPU speeds. Furthermore, this type of formulation is not amenable to a controls analysis since a transfer function or state-space representation for the CFD model is not explicitly defined.

When running a coupled aeroelastic simulation, it is the unsteady CFD solution at each time step which requires the overwhelming proportion of CPU time. Hence, recent research has targeted the acceleration of this solution through various modeling techniques. In particular, system identification has been shown to yield a significant savings in computational time for CFD-based aeroelastic analysis.¹

The system identification methodology allows one to develop an efficient mathematical model for the input-output relationship of an unsteady CFD solution. The system model then replaces the unsteady CFD solution in the coupled aeroelastic analysis resulting in a computationally efficient aeroelastic simulation while still retaining the accuracy of the original CFD model. This methodology has the advantage that it is applicable to a wide range of flow regimes, including transonic, and any arbitrary geometry. It will also be demonstrated that this methodology has the further advantage of allowing the problem to be recast in state-space form. The state matrices for the aeroelastic system can then be used for stability analysis by computing eigenvalues or for aeroservoelastic applications where control laws are implemented.

The emphasis of the present work is to further demonstrate the efficacy of using system identification techniques to accelerate CFD-based aeroelastic analysis for three-dimensional structures. The previously developed system identification procedure is summarized and an analysis is presented on selecting the optimum input signal for successful identification of the discrete-time model parameters. A derivation of the state-space form for the coupled aeroelastic system is presented along with the procedure for identifying aeroelastic instabilities from the resulting state matrices. Results are presented which address the extent to which this methodology is applicable to geometries and flows of practical interest in aerospace applications.

Computational Tools

Computational analysis for this study was performed using the aeroelastic capabilities of the STARS codes developed at NASA Dryden Flight Research Center. STARS² is an highly integrated, finite element based code for multidisciplinary analysis of flight vehicles including static and dynamic structural analysis, computational fluid dynamics, heat transfer, and aeroservoelastic capabilities.

Structural analysis in STARS is accomplished using the finite element method to compute the eigenvectors and eigenvalues which describe the elastic modes for a structure. Arbitrary motions of the structure can then be represented by multiplying each eigenvector by a generalized displacement and applying modal superposition. STARS unsteady CFD analysis is accomplished using a time-marched, finite element approach to solving the unsteady Euler equations. The CFD solution is performed on a mesh consisting of unstructured tetrahedra using the transpiration method to simulate structural deformations.

A complete aeroelastic analysis is accomplished by coupling a dynamics solver, using the modal vectors, with the unsteady CFD solver which computes the generalized aerodynamic forces acting on the structure. The coupled solution is then a time marched methodology for solving Equation (1), the matrix equation of motion for an arbitrary structure using generalized coordinates.

$$[\mathbf{M}]\ddot{\mathbf{q}} + [\mathbf{C}]\dot{\mathbf{q}} + [\mathbf{K}]\mathbf{q} = \mathbf{f}_a(t) \quad (1)$$

Considering the described solution scheme, the STARS aeroelastic solution method can be graphically represented by the simple block diagram shown in Figure 1.

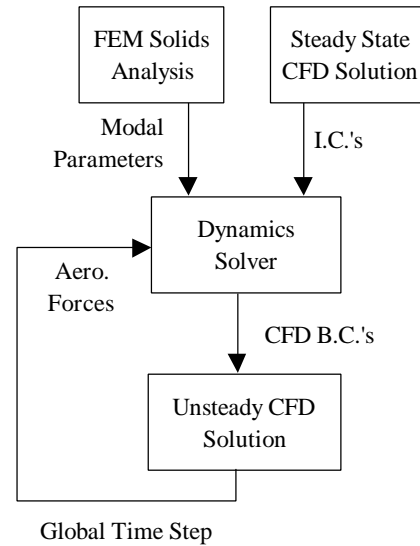


Figure 1: Block Diagram Representation of STARS Aeroelastic Solution

Notice in Figure 1 that aeroelastic solution scheme requires two initial pieces of information about the problem; modal parameters for the structure and a steady state CFD solution. The modal parameters define the structural dynamics of the problem, and the steady state CFD solution assures the time accuracy of the unsteady CFD solution by providing it with initial starting conditions. These two items are required for any problem before beginning an aeroelastic analysis.

System Identification Procedure

As shown in Figure 2, it is the unsteady CFD solution at each time step which requires the overwhelming proportion of CPU time when implementing the described aeroelastic solution scheme. In an effort to make CFD-based aeroelastic analysis more practical in an operational environment, a system identification procedure has been developed

which allows one to develop an efficient mathematical model which closely approximates the aerodynamics predicted by the unsteady CFD solution. This aerodynamic model is then independent of the structural parameters and can be used to search for aeroelastic instabilities by varying the dynamic pressure, generalized mass, etc.

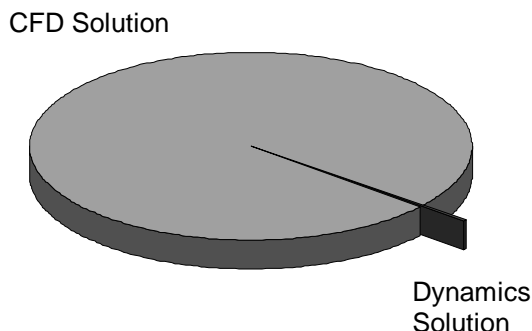


Figure 2: Typical CPU Fraction During STARS Aeroelastic Analysis

The system identification procedure makes the assumption that most aeroelastic systems can be treated as dynamically linear. That is, the aerodynamics respond linearly to small perturbations about a potentially nonlinear steady-state mean flow. This assumption is supported by modern aeroelastic research which indicates that it is the static nonlinearities which are important in an aeroelastic analysis.³ Furthermore, this assumption requires no extra computational effort since the nonlinear steady state solution is already required for all problems.

By borrowing from Figure 1, one can represent the STARS unsteady CFD solver as a simple dynamic system using the block diagram of Figure 3. Notice that the unsteady CFD solution is a multi-input multi-output, MIMO, system with an input vector consisting of generalized displacements for the structure and an output vector consisting of generalized aerodynamic forces.

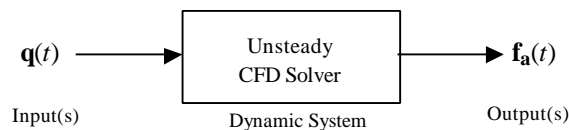


Figure 3: Block Diagram Representation of STARS Unsteady CFD Solver

In order to model the input-output relationship for this MIMO system, the system identification procedure utilizes a vector form of the discrete-time ARMA model structure as defined by Equation (2).

$$\mathbf{f}_a(k) = \sum_{i=1}^{na} [\mathbf{A}_i] \mathbf{f}_a(k-i) + \sum_{i=0}^{nb-1} [\mathbf{B}_i] \mathbf{q}(k-i) \quad (2)$$

Notice that the ARMA model structure of Equation (2) equates the current output, or generalized aerodynamic force, to a linear combination of na past outputs and nb past inputs of the unsteady CFD solver. Hence, a model order, or size, can be defined using these two integers, $na-nb$.

With the model structure defined, system identification is then a process for computing the matrices of constant coefficients which will result in a model that accurately matches the real dynamics of the unsteady CFD solution for a particular flow field. The methodology implemented in STARS utilizes a least-squares numerical technique to compute the model coefficients which minimize the error between the model and a set of time history data, or “training” data, taken from the unsteady CFD solution. This training data is the aerodynamic response time history computed for a prescribed motion of the structure.

Once an optimum fit to the training data is identified, the model can then be implemented to predict the aerodynamics for any arbitrary motion of the structure. By implementing it in place of the unsteady CFD solution in a coupled aeroelastic analysis, one can predict complete aeroelastic time histories in a fraction of the time while still retaining the accuracy of the original CFD solution. Furthermore, the aerodynamic model may be used repeatedly with various combinations of structural parameters to predict aeroelastic instabilities since it was developed independent of the structural dynamics for the problem. The model must only be retrained when the flow physics of the problem are altered by changing the Mach number.

Input Optimization

The success of any system identification procedure is highly dependent on the amount and quality of time history data available when identifying the model’s parameters. There must be as much information about the system’s dynamics as possible packed into the training set of data in order for the identification procedure to succeed. Hence, the prescribed input signal used in the initial set of training data must be chosen carefully.

When choosing the training input, conventional wisdom indicates that it should excite a broad spectrum of frequencies in the dynamic system. Hence the harmonic content of the input should be examined to ensure it is suitable.⁸ For a system such as an unsteady CFD solver, one has very careful control over the inputs, so an almost unlimited amount of signals are

available. The only limitation is that the input must be mathematically describable in terms of the boundary conditions for the flow solver so that the flow physics are accurately represented.

Although the aerodynamic model of Equation (2) only considers generalized displacements, another vector of generalized velocities is also needed to complete the boundary conditions required for a CFD solution. Furthermore, it is required that there be mathematical consistency between the two set of boundary conditions or the flow physics will not be accurately represented. That is, integrating the velocity input must yield the displacement input, and differentiating the displacement input must yield the velocity input. If this condition is not met, one will derive an aerodynamic model which has improper physics and cannot be used to model an aeroelastic problem.

Historically, the 3211 multistep input has been widely utilized in flight testing applications of system identification. In addition to being easy to implement, the 3211 multistep has a broad frequency content packed into a short signal. After evaluating a variety of input signals with the unsteady CFD solution, the 3211 multistep was initially chosen as the optimum input for system identification. However, the multistep input was implemented in an unorthodox way in order to satisfy the conditions required for mathematical consistency between the CFD boundary conditions.

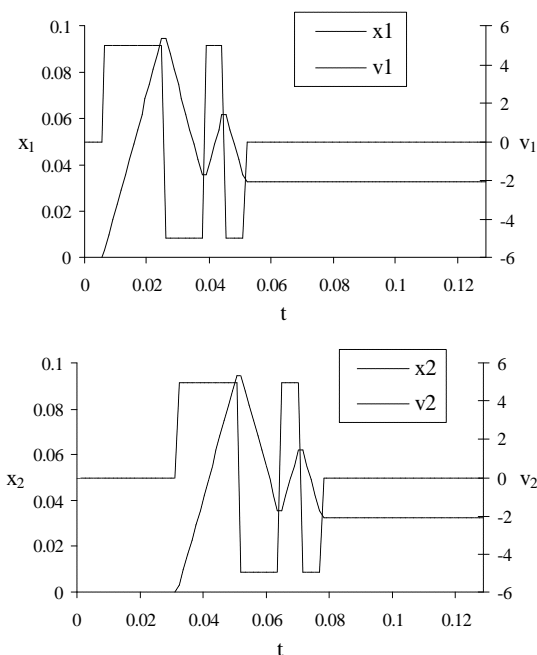


Figure 4: 3211 Multistep Input Signal for Unsteady CFD Flow Solver

As seen in Figure 4, the 3211 multistep was applied to the velocity boundary condition and then integrated to compute the displacement boundary condition. Implementing the multistep in this way resulting in two interesting boundary condition time histories and avoided the mathematical discontinuities that would have appeared in the velocity boundary condition if the multistep had been applied to the displacements and differentiated. Furthermore, notice that the multistep inputs for each mode are applied out of phase to allow the identification procedure to identify the dynamic effects of each unique input in the time history data.

To date, this multistep input has been utilized on a variety of aeroelastic problems and yields models which are typically in excellent agreement with the unsteady CFD solution.^{1,11} However, slight instabilities which do not exist in the unsteady CFD solution were sometimes observed at high frequencies for these models. Hence, more recent work has relied on a reworked multistep input which has a better frequency content to aid in the identification of the higher frequency dynamics. As with the 3211 multistep, the variable amplitude multistep, Figure 5, is applied to the velocity boundary condition, and its integral, Figure 6, is applied to the displacement boundary condition.

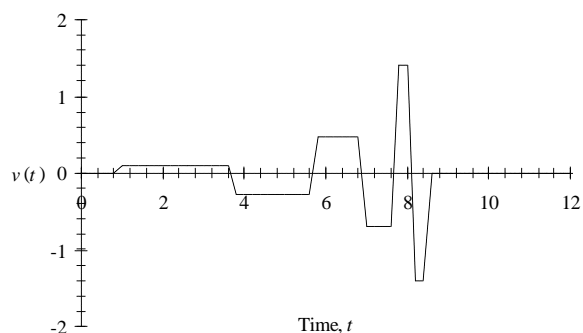


Figure 5: Variable Amplitude Multistep Input

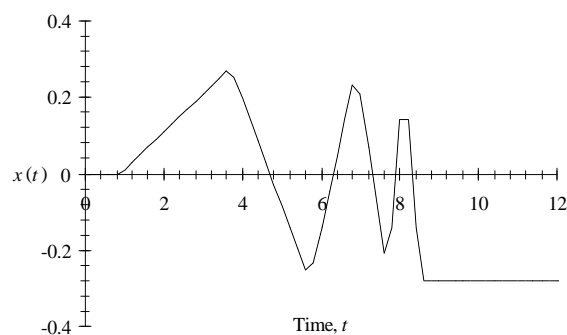


Figure 6: Integral of Variable Amplitude Multistep Input

The amplitudes for each step of the new input are chosen such that the area under each step remains constant. Additionally, the length of each step is chosen such that the total length of the variable amplitude multistep is the same as the previously implemented 3211 multistep. For comparison between the frequency content of the two inputs, the power spectral density, PSD, for each displacement time history is plotted versus the ratio between actual frequency and critical frequency, f / f_c , in Figure 7. Notice that there is an order of magnitude improvement in frequency content for the variable amplitude multistep across the entire frequency range. In particular, the increased power at high frequencies helps to eliminate the model instabilities previously observed when using the 3211 multistep for system identification.

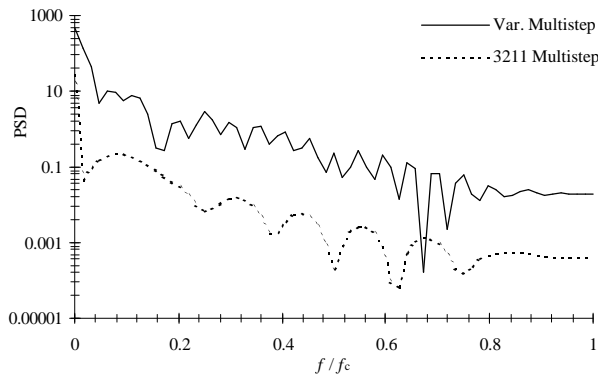


Figure 7: Comparison Between Power Spectral Density for Displacement Inputs

State-Space Representation

After completing the system identification procedure, one then has an explicit mathematical model for the aerodynamic response of the structure. This discrete-time aerodynamic model takes the place of the unsteady CFD solution in the coupled aeroelastic solution. The resulting aeroelastic model can be used to predict complete response time histories in seconds rather than the days one would wait when employing the unsteady CFD solution. Hence the search for aeroelastic instabilities, or the crossover from stable to divergent time histories, may be completed by varying the dynamic pressure and re-executing the aeroelastic simulation at almost no computational cost.

However, it is often difficult to pin down an aeroelastic instability by examining response time histories, especially for a structure with multiple mode shapes. The interaction between different structural modes often results in erratic response time histories such as that shown in Figure 8 which was taken from a

six mode testcase. The time history shown in Figure 8 is obviously not divergent, however it is not obvious how to estimate the damping ratio or quantify how close the point of instability is. Hence, the search for instabilities in the aeroelastic system becomes the task of making qualitative comparisons between obviously stable and divergent time histories in order to estimate where the crossover point would be.

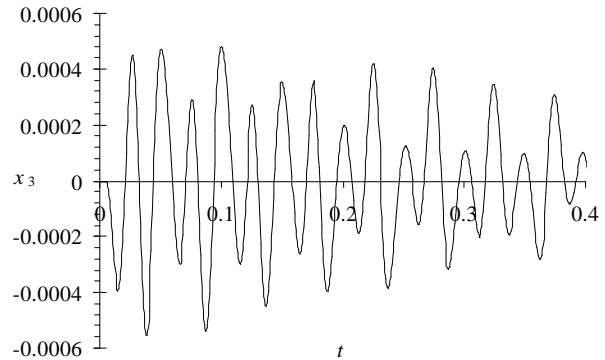


Figure 8: Individual Response Time History From a Six Mode Testcase

Rather than studying time history data in the search for instabilities, one could instead transform the problem into state-space form and compute its eigenvalues by taking advantage of now having an explicit mathematical model for the aerodynamics of the system. Notice in Figure 1 that the STARS aeroelastic solution method essentially consists of two discrete-time systems coupled together in a linear feedback loop. Now that an explicit representation for the unsteady CFD solution exists, one can collapse this system into a coupled state-space form by connecting the inputs and outputs of the two systems and simplifying.

The first step in the aeroelastic state-space formulation is to derive the state matrices for each individual system; the structural dynamics and aerodynamics. One might be tempted to derive the transfer function form for the two systems and use block diagram algebra to simplify them into a single closed-loop transfer function, however this is not convenient for complicated MIMO systems as it is difficult to automate generically in a computer algorithm.

First, consider the structural dynamics model implemented by STARS. As discussed previously, STARS solves Equation (1), the matrix equation of motion for an arbitrary structure in generalized coordinates. Note that the force vector on the right-hand side of Equation (1) can be any forcing function for the structural system, not just an aerodynamic

forcing function. Hence, the aerodynamic subscript will be dropped in the derivation of the structural system in favor of allowing any generic forcing function, $\mathbf{f}(t)$, to act on the system. The state space form for the structural equation of motion can then be shown to be as follows:

$$\dot{\mathbf{x}}_s(t) = [\mathbf{A}_s] \mathbf{x}_s(t) + [\mathbf{B}_s] \mathbf{f}(t) \quad (3)$$

$$\mathbf{q}(t) = [\mathbf{C}_s] \mathbf{x}_s(t) + [\mathbf{D}_s] \mathbf{f}(t) \quad (4)$$

where...

$$\mathbf{x}_s(t) \equiv \begin{Bmatrix} \dot{\mathbf{q}}(t) \\ \mathbf{q}(t) \end{Bmatrix} \quad [\mathbf{A}_s] = \begin{bmatrix} -[\mathbf{M}]^{-1}[\mathbf{C}] & -[\mathbf{M}]^{-1}[\mathbf{K}] \\ [\mathbf{I}] & [0] \end{bmatrix}$$

$$[\mathbf{B}_s] = \begin{bmatrix} [\mathbf{M}]^{-1} \\ [0] \end{bmatrix} \quad [\mathbf{C}_s] = \begin{bmatrix} [0] & [\mathbf{I}] \end{bmatrix} \quad [\mathbf{D}_s] = [0]$$

These matrix equations are solved numerically in STARS using a state transition matrix solution. This solution methodology is the discrete-time equivalent of applying a zero-order hold to the input and sampling the output of the original continuous-time system as shown in Figure 9.

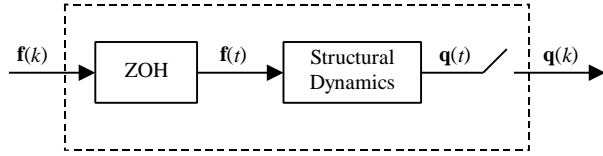


Figure 9: Block Diagram Representation of Equivalent Discrete-Time Structure

With this in mind, one can convert the above continuous-time system, Equations (3) and (4), to its discrete-time equivalent as follows:

$$\mathbf{x}_s(k+1) = [\mathbf{G}_s] \mathbf{x}_s(k) + [\mathbf{H}_s] \mathbf{f}(k) \quad (5)$$

$$\mathbf{q}(k) = [\mathbf{C}_s] \mathbf{x}_s(k) + [\mathbf{D}_s] \mathbf{f}(k) \quad (6)$$

where...

$$[\mathbf{G}_s] = e^{[\mathbf{A}_s] \Delta t}$$

$$[\mathbf{H}_s] = \left(\int_0^{\Delta t} e^{[\mathbf{A}_s] I} dI \right) [\mathbf{B}_s] = (e^{[\mathbf{A}_s] \Delta t} - [\mathbf{I}]) [\mathbf{A}_s]^{-1} [\mathbf{B}_s]$$

Next, consider the discrete-time aerodynamic model obtained using the system identification procedure. As seen in Figure 3, this model maps the relationship between generalized displacements and generalized aerodynamic forces. The unsteady CFD solver in STARS uses the free stream dynamic pressure as a linear scaling factor for converting from the CFD

unknowns into the surface pressure needed to compute generalized forces. Hence, the discrete-time aerodynamic model that has been developed for generalized forces can be implemented independent of the dynamic pressure by scaling it to match whichever current dynamic pressure is desired.

Based on the definition of dynamic pressure, Equation (7), one typically uses the free stream density as the model scaling parameter since the Mach number must be held constant for a given model.

$$q = \frac{1}{2} \rho (M \cdot a)^2 \quad (7)$$

For convenience, we then define a scaled aerodynamic force, $\hat{\mathbf{f}}_a(k)$, which has the initial training density, $\hat{\rho}$, divided out. This scaled aerodynamic force is related to the original aerodynamic force the model was trained to predict by Equation (8).

$$\mathbf{f}_a(k) = \hat{\rho} \hat{\mathbf{f}}_a(k) \quad (8)$$

By substituting this relationship into the aerodynamic model of Equation (2) and rearranging, the new equation for the properly scaled aerodynamic model is given by Equation (9). When implementing this model in an aeroelastic problem, one must simply multiply by the desired free stream density to get the correct aerodynamic force.

$$\hat{\mathbf{f}}_a(k) = \sum_{i=1}^{na} [\mathbf{A}_i] \hat{\mathbf{f}}_a(k-i) + \frac{1}{\hat{\rho}} \sum_{i=0}^{nb-1} [\mathbf{B}_i] \mathbf{q}(k-i) \quad (9)$$

In order to derive the state-space form for this model, we define a state-vector, $\mathbf{x}_a(k)$, consisting of $(na + nb - 1)$ vector states as follows:

$$\mathbf{x}_a(k) = \begin{Bmatrix} \hat{\mathbf{f}}_a(k-1) \\ \vdots \\ \hat{\mathbf{f}}_a(k-na) \\ \mathbf{q}(k-1) \\ \vdots \\ \mathbf{q}(k-nb+1) \end{Bmatrix} \quad (10)$$

The state space form for the discrete-time aerodynamic model can then be shown to be as follows:

$$\mathbf{x}_a(k+1) = [\mathbf{G}_a] \mathbf{x}_a(k) + [\mathbf{H}_a] \mathbf{q}(k) \quad (11)$$

$$\hat{\mathbf{f}}_a(k) = [\mathbf{C}_a] \mathbf{x}_a(k) + [\mathbf{D}_a] \mathbf{q}(k) + \hat{\mathbf{f}}_0 \quad (12)$$

where...

$$\begin{aligned}
 [\mathbf{G}_a] &= \begin{bmatrix} [\mathbf{A}_1] & [\mathbf{A}_2] & \cdots & [\mathbf{A}_{na-1}] & [\mathbf{A}_{na}] & \frac{1}{F}[\mathbf{B}_1] & \frac{1}{F}[\mathbf{B}_2] & \cdots & \frac{1}{F}[\mathbf{B}_{nb-2}] & \frac{1}{F}[\mathbf{B}_{nb-1}] \\ [\mathbf{I}] & [0] & \cdots & [0] & [0] & [0] & [0] & \cdots & [0] & [0] \\ [0] & [\mathbf{I}] & \cdots & [0] & [0] & [0] & [0] & \cdots & [0] & [0] \\ \vdots & \vdots & \ddots & \vdots & \vdots & \vdots & \vdots & \ddots & \vdots & \vdots \\ [0] & [0] & \cdots & [\mathbf{I}] & [0] & [0] & [0] & \cdots & [0] & [0] \\ [0] & [0] & \cdots & [0] & [0] & [0] & [0] & \cdots & [0] & [0] \\ [0] & [0] & \cdots & [0] & [0] & [\mathbf{I}] & [0] & \cdots & [0] & [0] \\ [0] & [0] & \vdots & [0] & [0] & [0] & [\mathbf{I}] & \cdots & [0] & [0] \\ \vdots & \vdots & \ddots & \vdots & \vdots & \vdots & \vdots & \ddots & \vdots & \vdots \\ [0] & [0] & \cdots & [0] & [0] & [0] & [0] & \cdots & [\mathbf{I}] & [0] \end{bmatrix} & [\mathbf{H}_a] = \begin{bmatrix} \frac{1}{F}[\mathbf{B}_0] \\ [0] \\ [0] \\ \vdots \\ [0] \\ [\mathbf{I}] \\ [0] \\ [0] \\ \vdots \\ [0] \end{bmatrix} \\
 [\mathbf{C}_a] &= [[\mathbf{A}_1] \quad [\mathbf{A}_2] \quad \cdots \quad [\mathbf{A}_{na-1}] \quad [\mathbf{A}_{na}] \quad \frac{1}{F}[\mathbf{B}_1] \quad \frac{1}{F}[\mathbf{B}_2] \quad \cdots \quad \frac{1}{F}[\mathbf{B}_{nb-2}] \quad \frac{1}{F}[\mathbf{B}_{nb-1}]] & [\mathbf{D}_a] &= \frac{1}{F}[\mathbf{B}_0]
 \end{aligned}$$

Notice in Equation (12) that the output for the discrete-time aerodynamic model includes a vector of static offsets, $\hat{\mathbf{f}}_0$. These are the scaled static offsets subtracted from the aerodynamic time history data in the de-trending process of the system identification procedure. To keep the state-space derivation consistent with the STARS aeroelastic solution scheme, this vector of static offsets must be added to the aerodynamics predicted by the system model. However, it will be seen later that the static offset vector is not important to the overall stability of the aeroelastic system.

With both the structural and aerodynamic systems now defined, the block diagram models from Figure 9 and Figure 3 are connected in a linear feedback loop as shown in Figure 10 below. To be consistent with the STARS numerical solution scheme, the aerodynamic forces are connected as negative feedback while an impulsive disturbance force, \mathbf{f}_1 , is introduced to excite the initial motion of the structure.

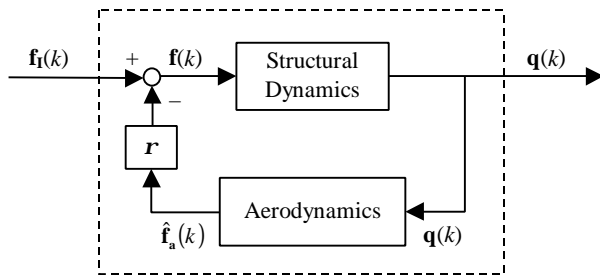


Figure 10: Block Diagram Representation of Coupled Aeroelastic System

Based on the layout of the system shown in Figure 10, a coupled aeroelastic system can be derived by first

substituting the output of the structural dynamics system, Equation (6), into the aerodynamics system, Equations (11) and (12). Next, the modified output equation for the aerodynamics system is substituted into the structural dynamics system, Equations (5) and (6). After some manipulation and simplification, the resulting coupled aeroelastic system in state-space form is defined in terms of the aerodynamics and structural dynamics state vectors as follows:

$$\begin{Bmatrix} \mathbf{x}_s(k+1) \\ \mathbf{x}_a(k+1) \end{Bmatrix} = [\mathbf{F}] \begin{Bmatrix} \mathbf{x}_s(k) \\ \mathbf{x}_a(k) \end{Bmatrix} + \begin{bmatrix} [\mathbf{H}_s] \\ [0] \end{bmatrix} \mathbf{f}_1(k) - \begin{Bmatrix} \mathbf{r}[\mathbf{H}_s] \hat{\mathbf{f}}_0 \\ [0] \end{Bmatrix} \quad (13)$$

$$\mathbf{q}(k) = \begin{bmatrix} [\mathbf{C}_s] & [0] \end{bmatrix} \begin{Bmatrix} \mathbf{x}_s(k) \\ \mathbf{x}_a(k) \end{Bmatrix} \quad (14)$$

where...

$$[\mathbf{F}] \equiv \begin{bmatrix} [\mathbf{G}_s] - \mathbf{r}[\mathbf{H}_s][\mathbf{D}_a][\mathbf{C}_s] & -\mathbf{r}[\mathbf{H}_s][\mathbf{C}_a] \\ [\mathbf{H}_a][\mathbf{C}_s] & [\mathbf{G}_a] \end{bmatrix} \quad (15)$$

Stability Analysis

With the coupled state-space model for the aeroelastic system now defined, it is possible to directly evaluate the stability of the system without examining multiple sets of time history data. Instead, one can turn to discrete-time stability criteria and examine the roots, or eigenvalues, of the aeroelastic system in order to evaluate its stability. Hence, the aeroelastic stability criteria for this discrete-time system is then that all eigenvalues of the matrix defined by Equation (15) lie within the unit circle when plotted in the complex plane.

The task at hand is then to produce a root locus by computing the eigenvalues for the aeroelastic state-matrix at various densities. To accomplish this task, a matrix eigenvalue solver is employed which computes the $nr \times (na + nb + 1)$ eigenvalues for the previously defined state matrix. To date, this methodology has been used successfully to predict aeroelastic instabilities for several geometries over a wide range of Mach numbers.

One such geometry is the AGARD 445.6 wing configuration which is a standard aeroelastic test case that has been investigated experimentally in the Langley Transonic Dynamics tunnel. A planform view of the configuration is shown in Figure 11. This wing geometry is often used in the literature as a validation case for computational aeroelastic codes in the transonic flow regime. Recent work has shown that the STARS aeroelastic analysis module is capable of predicting the experimental data for this wing geometry including the transonic dip in the flutter boundary around Mach 1.0.¹⁰

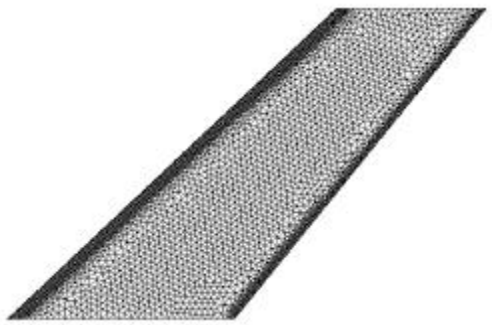


Figure 11: AGARD 445.6 Test Wing Geometry and Surface Discretization

In STARS, the AGARD is modeled structurally using the two dominant eigenvectors which represent the first two natural vibration modes of the structure. These mode shapes physically represent wing first bending and torsion. The CFD mesh for the AGARD consists of 70,036 nodes and 376,125 tetrahedral elements.

To begin the aeroelastic analysis of the AGARD wing configuration, the system identification procedure previously discussed was used to develop a discrete-time aerodynamic model for the unsteady CFD solution at Mach 0.96. During the identification procedure, a 4-10 model order yielded the best agreement with the CFD training data and was chosen as the optimum model. With an explicit aerodynamic model available for the AGARD at Mach 0.96, the coupled aeroelastic state matrix define by Equation (15) was assembled for this system by following the previously derived procedure. This resulted in 30×30 matrix which is a function of the free stream density.

A root locus for the AGARD aeroelastic system can then be developed by computing the 30 eigenvalues for the state matrix over a range of densities. Figure 12 presents the AGARD root locus plot produced using ten evenly spaced density values ranging from 1.4×10^{-9} to 5.0×10^{-9} slinches/in³. Using this plot, aeroelastic instabilities can be identified by searching for eigenvalues which cross the unit circle, or whose magnitude is greater than one. As seen in the plots below, the first instability occurs near a density of 3.2×10^{-9} slinches/in³.

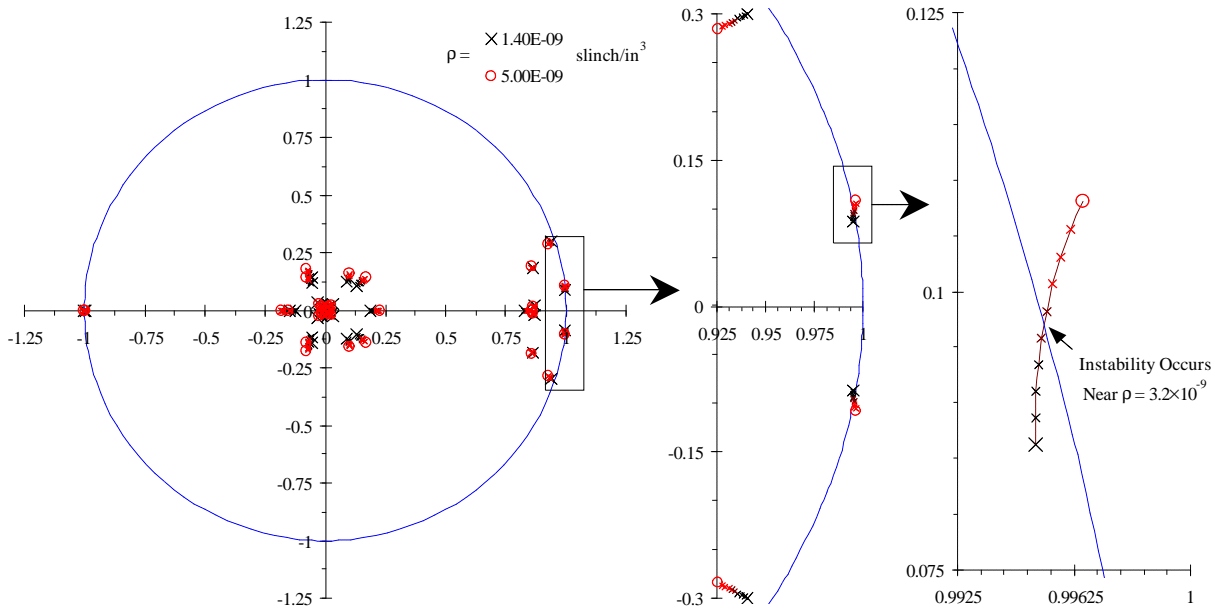


Figure 12: Complete Root Locus for AGARD Discrete-time Aeroelastic System at Mach 0.96 Including Close-ups of the Instability Crossover Point

To validate the observed instability is correct, one can return to the time history analysis typical used in the STARS aeroelastic analysis. Both the discrete-time model and the unsteady CFD solution were used to predict the aeroelastic time histories for the AGARD at Mach 0.96 and the instability crossover density of 3.2×10^{-9} slinches/in³. As seen in Figure 13, both the model and CFD solutions are in excellent agreement and both solutions seem to have predicted neutrally stable or undamped time histories. This proves that the aerodynamic model is an accurate representation of the unsteady CFD solution and that the state-space stability analysis is capable of accurately capturing aeroelastic instabilities.

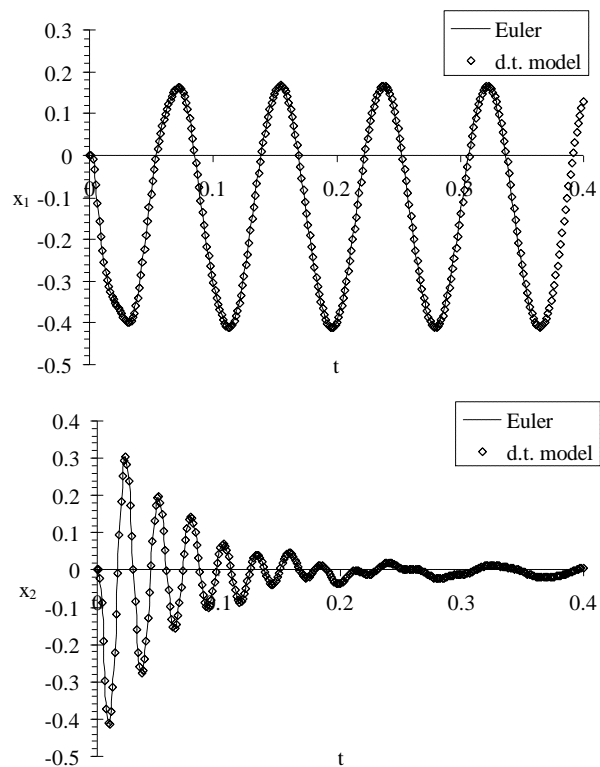


Figure 13: Comparison Between Model and Euler Aeroelastic Time Histories for the AGARD at Mach 0.96 and $\rho = 3.2 \times 10^{-9}$

Aside from the benefit of being able to accurately quantify aeroelastic instabilities, the state-space stability analysis provides further insight into the physics of an aeroelastic system not readily available using time history analysis. For the two mode AGARD system, we see that there are two dominant eigenvalues along the right-hand edge of the unit circle. Notice that as the density increases, one of these roots moves inward and becomes more stable while the other root moves outward until it finally destabilizes. Furthermore, we recognize that the unstable root is actually the lowest frequency mode for the system. As seen in Figure 14, the generalized displacements for each mode of the AGARD follow divergent paths beyond the instability density. However, we now know from the state-space stability analysis that it is mode one which drives these divergent time histories.

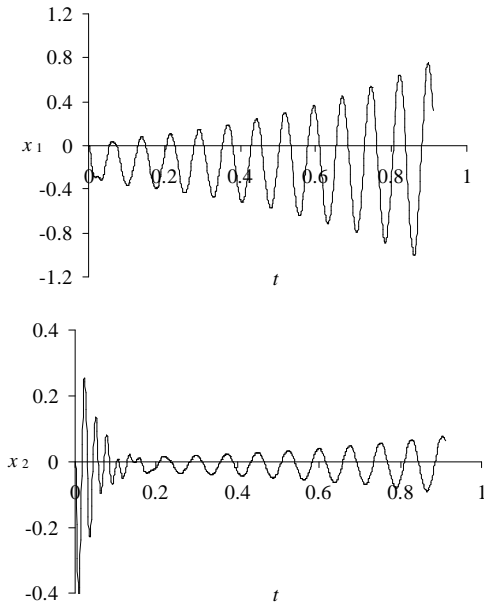


Figure 14: Unstable Time Histories For AGARD Aeroelastic System at Mach 0.96

Another interesting geometry to study is that of the Generic Hypersonic Vehicle (GHV). The GHV is a testcase developed by NASA to test the aeroelastic effects that might be observed on a hypersonic vehicle. Figure 15 shows the CFD surface mesh used to model the GHV. The CFD mesh for the GHV consists of 58,786 nodes and 323,417 tetrahedral elements.

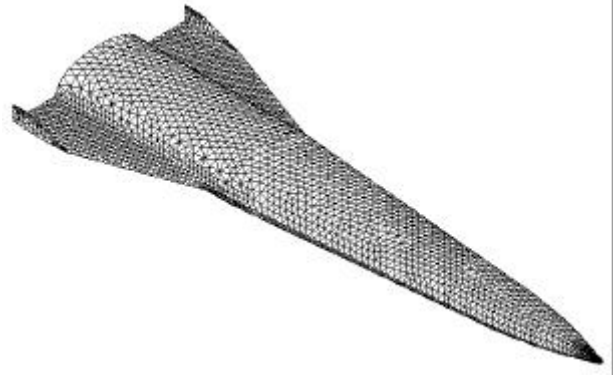


Figure 15: GHV Geometry and Surface Discretization

Structurally, the GHV is much more complicated than the AGARD as it is modeled using nine eigenvectors which represent various bending and torsion modes for both the wings and body. As with the AGARD system, the system identification procedure was used to develop a discrete-time model for the aerodynamics of the GHV at Mach 2.20. This time, a 2-11 model order yielded the best agreement between the aerodynamic model and the unsteady CFD training data. The resulting aeroelastic state was then defined by a 126×126 square matrix.

Figure 16 presents the GHV root locus plot produced using ten evenly spaced density values ranging from 1.4×10^{-7} to 5.0×10^{-7} slinches/in³. As before, we identify instabilities by searching for eigenvalues which cross the unit circle. As seen in the plots below, the first instability occurs near a density of 2.6×10^{-7} slinches/in³ and a second crossover occurs later at a density near 3.4×10^{-7} slinches/in³. Although the second instability is of no practical interest since the first instability is critical and would most likely result in the destruction of the vehicle, it is interesting to note that the second instability does exist and can be quantified using the state-space analysis. For even more complicated systems, one might find this information more useful if eigenvalues happen to become unstable and then loop back inside the unit circle, making the higher order instabilities more critical.

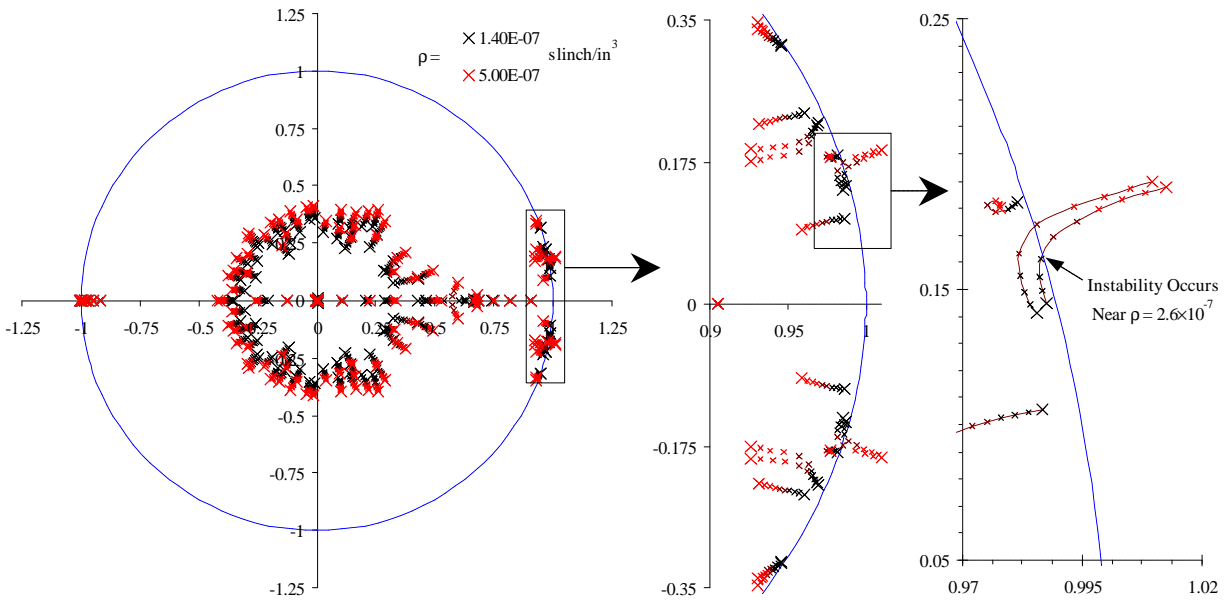


Figure 16: Complete Root Locus for GHV Discrete-time Aeroelastic System at Mach 2.20 Including Close-up of Unstable Crossover Point

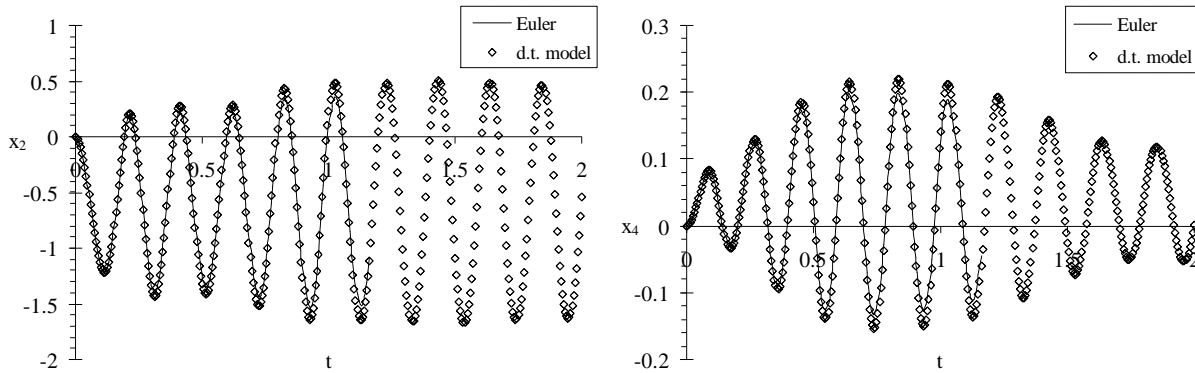


Figure 17: Comparison Between Model and Euler Aeroelastic Time Histories for Mode 2 & 4 of the GHV at Mach 2.20 and $\rho = 2.6 \times 10^{-7}$ slinches/in³

As with the AGARD, we validate the observed instability by comparing the aeroelastic time histories predicted by the discrete-time model and the unsteady CFD solution at Mach 2.20 and the instability crossover density of 2.6×10^{-7} slinches/in³. As seen in Figure 17, both the model and CFD solutions are in excellent agreement for modes two and four and both solutions predict time histories near, but slightly below the actual neutral point. Note that only modes two and four are shown here to conserve space, but results are similar for all nine modes. Again, this proves that the aerodynamic model is an accurate representation of the unsteady CFD solution for the GHV and that the state-

space stability analysis is capable of accurately capturing its aeroelastic instabilities.

Conclusions

The objective of this study was to develop an accurate and efficient method discrete-time aerodynamic model for use in CFD-based aeroelastic analysis. The system identification methodology presented here has the benefit that only one unsteady CFD solution is required to produce a model for each Mach number, resulting in a substantial saving in computational time for aeroelastic analysis. The technique is applicable to different structural

geometries over a wide range of Mach numbers including the transonic regime.

The system identification methodology has the further benefit of providing an explicit mathematical model for the unsteady CFD solution which then allows one to develop a state-space form the aeroelastic system. With a state-space form defined, aeroelastic instabilities are easier to quantify using discrete-time stability analysis based on the eigenvalues of the system. Although not demonstrated here, the state-space form is also better suited for aeroservoelastic applications as well. For such an application, a control law could be coupled around the aeroelastic system making a controls analysis more efficient.

Based on the benefits demonstrated here, this approach may make the use of CFD simulations routine in the aeroelastic analysis of aerospace vehicles.

Acknowledgements

Funds for the support of this study have been allocated through the NASA-Ames University Consortium Office, under Interchange Number NCC2-5105, and Oklahoma State University.

References

1. Cowan, T.J., Arena, A.S., and Gupta, K.K., "Accelerating CFD-Based Aeroelastic Predictions Using System Identification," AIAA-98-4152, August, 1998.
2. Gupta, K.K., "STARS – An Integrated General-Purpose Finite Element Structural, Aeroelastic, and Aeroservoelastic Analysis Computer Program," NASA TM-4795, May 1997.
3. Dowell, E.H., et al, *A Modern Course in Aeroelasticity*, 3rd Revised and Enlarged Edition, Kluwer Academic Publishers, 1995.
4. Ljung, L., *System Identification: Theory For The User*, Prentice Hall, Inc., New Jersey, 1987.
5. Hollkamp, J. J. and Batill, S. M., "Automated Parameter Identification and Order Reduction for Discrete Time Series Models", *AIAA Journal*, Vol. 29, No. 1, 1991, pp. 96-103.
6. Pinkelman, J. K., Batill, S. M., and Kehoe, M. W. "Total Least Squares Criteria in Parameter Identification for Flight Flutter Testing," *Journal of Aircraft*, Vol. 33, No. 4, 1996, pp. 784-792.
7. Hollkamp, J. J., and Batill, S. M., "A Recursive Algorithm For Discrete Time Domain Parameter Identification," AIAA Paper 90-26805.
8. Hamel, P. G., and Jategaonkar, R. V., "Evolution of Flight Vehicle System Identification," *Journal Of Aircraft*, Vol. 33, No. 1, 1996, pp. 9-28.
9. Press, W.H., Teukolsky, S.A., Vetterling, W.T., and Flannery, B.P., *Numerical Recipes in Fortran 77: The Art of Scientific Computing*, 2nd Edition, Cambridge University Press, 1992.
10. Gupta, K.K., "Development of a Finite Element Aeroelastic Analysis Capability," *Journal of Aircraft*, Vol. 33, No. 5, September-October 1996, pp. 995-1002.
11. Cowan, T.J., "Efficient Aeroelastic CFD Predictions Using System Identification," *Masters Thesis*, Oklahoma State University, May 1998.